JOURNAL OF SPACECRAFT AND ROCKETS
Vol. 43, No. 1, January–February 2006

Engineering Notes

ENGINEERING NOTES are short manuscripts describing new developments or important results of a preliminary nature. These Notes should not exceed 2500 words (where a figure or table counts as 200 words). Following informal review by the Editors, they may be published within a few months of the date of receipt. Style requirements are the same as for regular contributions (see inside back cover).

Compound Solar Sail with Optical Properties: Models and Performance

Giovanni Mengali* and Alessandro A. Quarta†
University of Pisa, I-56122 Pisa, Italy

Introduction

UNLIKE conventional solar sails, in a compound spacecraft the functions of collecting and directing the solar radiation are separated. A large sun-pointing mirror (the collector) directs the incoming solar radiation onto a small mirror (the reflector). The reflector then directs the beam of radiation onto a second, directing mirror (the director), which is used to control the orientation of the force acting on the compound sailcraft. The reason for this arrangement is that the collector always faces the sun whatever the direction of thrust. Therefore, the collector completely exploits the solar light power and always provides the maximum obtainable thrust for a given area of the collector. This contrasts with the behavior of a flat sail model in which the orientation of the sail must be tilted at some angle α (the cone angle) with respect to the sun line to obtain the desired thrust direction. Clearly, the sail area, as seen by the sun, is decreased by an amount proportional to $\sin\alpha$. As a result, the force law for an ideal compound sail it is known to be proportional to $\cos\alpha$, whereas for a conventional sail it is proportional to $\cos^2\alpha$. Accordingly, a compound spacecraft is superior, in principle, to a conventional one.

The general arrangement of a compound sail, often referred to as solar photon thrustor, is described in a paper by Forward.[1] Assuming circular and coplanar planetary orbits, McInnes[2] discusses the minimum-time trajectories for interplanetary missions and makes a comparison between performance of conventional and compound sails. The general case of optimal control law for a three-dimensional problem has been recently derived by Mengali and Quarta,[3] and the application of a compound sail for Earth escape is treated in Ref. 4. Because the preceding papers assume perfectly reflecting surfaces, their results represent an upper bound to the achievable performance. However, when a realistic model of a conventional sail is used (which includes the optical and reradiation effects of the sail), the obtainable performance is known to be significantly worse than that predicted by an ideal model.[5] This problem is particularly important for a compound sail, where multiple reflections are needed to generate the desired thrust. The purpose of this Note is twofold: first, we aim at developing a suitable model of a compound sailcraft, which takes the optical properties of the various components into account. In doing so, we revisit and extend the results originally presented by Forward.[1] Second, we quantify the performance of the new model. To this end, we derive the minimum-time steering law of the nonideal compound sail for three-dimensional interplanetary trajectories and make a comparison with the results achievable with an ideal model.

Received 8 February 2005; revision received 9 June 2005; accepted for publication 9 June 2005.

*Associate Professor, Department of Aerospace Engineering; g.mengali@ing.unipi.it.

†Research Assistant, Department of Aerospace Engineering; a.quarta@ing.unipi.it.

System Description

The general arrangement of a compound solar sail is shown in Fig. 1. In the original paper by Forward,[1] this assembly of three mirrors is referred to as *dual reflector*. Recently, Flint[6] has revisited the compound solar-sail architecture. The basic components are the light collector, the reflector, the director, and a suitable structure connecting these three elements to each other and the payload. As suggested by Forward,[1] the whole system can be arranged such that the thrust vector passes through the center of mass of the whole system (including the payload) to avoid large disturbance torques.

The collector always faces the sun to expose the maximum area for sunlight collection. Its large surface is shaped into a lens-like form to concentrate the nearly parallel light rays in its optical focus. It is assumed[1] that the collector surface is a spherical cap with radius R_c and aperture angle ξ_0 (Fig. 1) measured from the collector optical axis. The collector optical focus is halfway to the center of curvature. To reduce the spherical aberration phenomenon, the light rays should be close to the collector optical axis. This amounts to saying that ξ_0 must be reasonably small.

The light rays reflected by the collector strike the reflector surface and are mirrored toward the director. The reflector is assumed to be a small, spherical surface whose optical focus coincides with that of the collector.

The director is a small, flat mirror whose center is mounted on the collector optical axis. The director can be tilted at a suitable angle to reflect the incoming light rays from the reflector and orient the resulting thrust in the desired direction. Both reflector and director

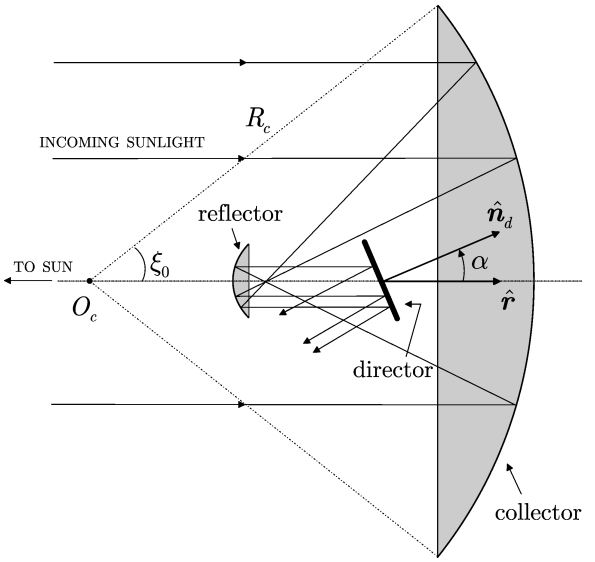

Fig. 1 Conceptual sketch of the compound solar sail (not to scale).

areas are much smaller than that of the collector (on the order of 1/100 or less). Note, however, that this ratio cannot be made arbitrarily small because of limitations on the tolerable temperature of both reflector and director.

In the ideal case, assuming perfect reflection and no losses in all of the surfaces, the forces acting on the collector and the reflector cancel, and the resulting force on the compound sail is normal to the director surface. On the other hand, a more realistic force model is obtained by introducing the optical properties of the compound sail components. In this new model, the thrust vector can be thought of as the sum of two forces: one normal to the director surface and the other parallel to the collector axis, as discussed in the next section.

Optical Force Model for a Compound Sail

To develop a suitable model for a nonideal compound sailcraft, we start considering a nonperfect flat solar sail of area A_s. When the reflectance, absorption, and emissivity of the sail film are taken into account, the force exerted on the solar sail by the solar radiation pressure is commonly referred to as optical force model. More precisely, let s be the fraction of photons that are specularly reflected by the sail, B_{fr} and B_b are the non-Lambertian coefficients of the front and back sail surfaces, ϵ_{fr} and ϵ_b the corresponding front and back emissivities, and $\rho < 1$ the reflection coefficient. The force acting on the solar sail can be written as[7]

$$\boldsymbol{f}_s = P A_s \cos\alpha [b_1 \hat{\boldsymbol{r}} + (b_2 \cos\alpha + b_3)\hat{\boldsymbol{n}}] \tag{1}$$

where $P = P(r)$ is the solar radiation pressure at a distance r, $\hat{\boldsymbol{r}}$ is the unit vector in the direction of the incident radiation from the sun, $\hat{\boldsymbol{n}}$ is the unit vector normal to the sail in the direction of thrust, and α is the sail cone angle (that is, the angle between $\hat{\boldsymbol{r}}$ and $\hat{\boldsymbol{n}}$). Also, the force coefficients b_1, b_2, and b_3 are defined as

$$b_1 \triangleq 1 - \rho s, \qquad b_2 \triangleq 2\rho s \tag{2}$$

$$b_3 \triangleq B_{\text{fr}}\rho(1-s) + (1-\rho)\frac{\epsilon_{\text{fr}} B_{\text{fr}} - \epsilon_b B_b}{\epsilon_{\text{fr}} + \epsilon_b} \tag{3}$$

Force Acting on the Collector

Assuming the collector shape is a spherical cap, the force acting on the collector is evaluated with the aid of Fig. 2. The differential area $\mathrm{d}A$ of the collector is given by

$$\mathrm{d}A = R_c^2 \sin\xi \,\mathrm{d}\theta \,\mathrm{d}\xi \tag{4}$$

where ξ is the cone angle of the differential area and $\theta \in [0, 2\pi]$ is the corresponding right ascension measured on a plane orthogonal to the collector axis from some fixed position. Let $\hat{\boldsymbol{n}}$ be the unit vector normal to $\mathrm{d}A$; then

$$\hat{\boldsymbol{n}} \cdot \hat{\boldsymbol{r}} = \cos\xi \tag{5}$$

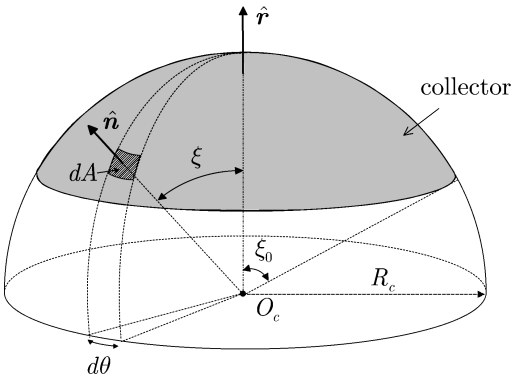

Fig. 2 Geometry of the collector.

where $\xi \in [0, \xi_0]$. From Eq. (1), the differential force $\mathrm{d}\boldsymbol{f}_c$ caused by photons, acting on the area $\mathrm{d}A$, is given by

$$\mathrm{d}\boldsymbol{f}_c = P\,\mathrm{d}A\cos\xi\left[b_{1_c}\hat{\boldsymbol{r}} + \left(b_{2_c}\cos\xi + b_{3_c}\right)\hat{\boldsymbol{n}}\right] \tag{6}$$

where b_{1_c}, b_{2_c}, and b_{3_c} are the force coefficients related to the optical properties of the collector reflecting film. For symmetry reasons, the resultant force acting on the collector is directed along the collector axis, which is parallel to $\hat{\boldsymbol{r}}$. Accordingly,

$$\boldsymbol{f}_c = \int_A \mathrm{d}\boldsymbol{f}_c = \hat{\boldsymbol{r}} \int_A \hat{\boldsymbol{r}} \cdot \mathrm{d}\boldsymbol{f}_c \tag{7}$$

Substituting Eqs. (4–6) into Eq. (7) and performing the integral yields

$$\boldsymbol{f}_c = (PA/12)\left[3b_{2_c}(1+\cos\xi_0)\left(1+\cos^2\xi_0\right)\right.$$
$$\left. + 4b_{3_c}\left(1+\cos\xi_0+\cos^2\xi_0\right) + 6b_{1_c}(1+\cos\xi_0)\right]\hat{\boldsymbol{r}} \tag{8}$$

where $A = 2\pi R_c^2(1-\cos\xi_0)$. It is useful to introduce the area A_p, which corresponds to the collector area projected on a plane normal to $\hat{\boldsymbol{r}}$. In other terms, A_p is the collector area as seen by the parallel light rays from the sun. Clearly, $A_p = \pi R_c^2 \sin^2\xi_0$ or $A/A_p = 2/(1+\cos\xi_0)$. Accordingly, Eq. (8) can be written as

$$\boldsymbol{f}_c = \frac{PA_p}{6}\left[3b_{2_c}\left(1+\cos^2\xi_0\right) + 4b_{3_c}\frac{1+\cos\xi_0+\cos^2\xi_0}{1+\cos\xi_0} + 6b_{1_c}\right]\hat{\boldsymbol{r}} \tag{9}$$

Force Acting on the Reflector

Because of the optical behavior, the light rays impinging on a differential area of the collector are in part reflected specularly, in part diffusively, and in part reemitted by thermal radiation from the collector. Assuming good optical properties of the collector surface, the fraction of photons specularly reflected is much greater than the fraction of those diffusively reflected and reradiated. (For instance, using Kapton coated with aluminum for the sail film, the specularly reflected photons are on the order of 80%.) Accordingly, to simplify the model it is assumed that the photons striking the reflector are just those specularly reflected by the collector.

The resultant force acting on the reflector $\boldsymbol{f}_r$ can be found using the same technique previously applied to the collector. The result is

$$\boldsymbol{f}_r = -\frac{P_r A_{r_p}}{6}\left[3b_{2_r}\left(1+\cos^2\xi_0\right)\right.$$
$$\left. + 4b_{3_r}\frac{1+\cos\xi_0+\cos^2\xi_0}{1+\cos\xi_0} + 6b_{1_r}\right]\hat{\boldsymbol{r}} \tag{10}$$

where b_{1_r}, b_{2_r}, and b_{3_r} are the force coefficients related to the optical properties of the reflector; A_{r_p} is the reflector area projected on a plane normal to $\hat{\boldsymbol{r}}$; and P_r is the corresponding radiation pressure. The latter can be evaluated as follows. The total power W_c striking the collector during the photon collection process is given by

$$W_c = PA_p c \tag{11}$$

where c is the speed of light. With an ideal collector, all of the power W_c would be completely redirected toward the reflector. However, because of the losses in the collector film, the power W_r striking the reflector is caused by the fraction of photons specularly reflected by the collector, that is,

$$W_r = \rho_c s_c W_c \tag{12}$$

where the subscript c refers to the collector characteristics. Because $W_r = P_r\, A_{r_p} c$, from Eqs. (11) and (12) one has

$$P_r A_{r_p} = PA_p \rho_c s_c \tag{13}$$

Substituting Eq. (13) into Eq. (10) yields

$$\boldsymbol{f}_r = -\frac{PA_p\rho_c s_c}{6}\left[3b_{2_r}\left(1+\cos^2\xi_0\right) + 4b_{3_r}\frac{1+\cos\xi_0+\cos^2\xi_0}{1+\cos\xi_0} + 6b_{1_r}\right]\hat{\boldsymbol{r}} \tag{14}$$

Assuming a collector with ideal optical properties ($\rho_c s_c = 1$), it turns out that $\boldsymbol{f}_r = -\boldsymbol{f}_c$. This confirms that in an ideal case the forces acting on the collector and the reflector cancel.

Force Acting on the Director

The force $\boldsymbol{f}_d$ acting on the director is calculated bearing in mind that this component is simply a flat-shaped mirror. From Eq. (1) one has

$$\boldsymbol{f}_d = P_d A_d \cos\alpha\left[b_{1_d}\hat{\boldsymbol{r}} + \left(b_{2_d}\cos\alpha + b_{3_d}\right)\hat{\boldsymbol{n}}_d\right] \tag{15}$$

where b_{1_d}, b_{2_d}, and b_{3_d} are the force coefficients related to the optical properties of the director; $\hat{\boldsymbol{n}}_d$ is the unit vector normal to the director; and α is the corresponding cone angle (see Fig. 1). The power striking the director is $W_d = P_d A_d c\cos\alpha$. Assuming it is only caused by the fraction of photons specularly reflected by the reflector, one obtains $W_d = \rho_r s_r W_r$. With the aid of Eq. (12), one has

$$P_d A_d \cos\alpha = PA_p\rho_c s_c \rho_r s_r \tag{16}$$

from which

$$\boldsymbol{f}_d = PA_p\rho_c s_c\rho_r s_r\left[b_{1_d}\hat{\boldsymbol{r}} + \left(b_{2_d}\cos\alpha + b_{3_d}\right)\hat{\boldsymbol{n}}_d\right] \tag{17}$$

Resultant Force and Sailcraft Acceleration

The resultant force acting on the spacecraft is the vector sum of the contributions by the collector, reflector, and director, that is,

$$\boldsymbol{f} = \boldsymbol{f}_c + \boldsymbol{f}_r + \boldsymbol{f}_d \tag{18}$$

The corresponding sailcraft acceleration $\boldsymbol{a}$ is simply $\boldsymbol{f}$ divided by the total spacecraft mass m. Substituting Eqs. (9), (14), and (17) into Eq. (18) and collecting the various terms yields

$$\boldsymbol{a} = (PA_p/m)[\mathcal{A}\hat{\boldsymbol{r}} + (\mathcal{B}\cos\alpha + \mathcal{C})\hat{\boldsymbol{n}}_d] \tag{19}$$

where

$$\mathcal{A} \triangleq \frac{1}{6}\left[3b_{2_c}\left(1-\frac{b_{2_r}}{2}\right)\left(1+\cos^2\xi_0\right) + 4\left(b_{3_c}-\frac{b_{2_c}b_{3_r}}{2}\right)\times\frac{\left(1+\cos\xi_0+\cos^2\xi_0\right)}{1+\cos\xi_0} + 6\left(b_{1_c}-\frac{b_{2_c}b_{1_r}}{2}\right)\right] + \frac{b_{2_c}b_{2_r}b_{1_d}}{4} \tag{20}$$

$$\mathcal{B} \triangleq \frac{b_{2_c}b_{2_r}b_{2_d}}{4}, \qquad \mathcal{C} \triangleq \frac{b_{2_c}b_{2_r}b_{3_d}}{4} \tag{21}$$

In Eqs. (20) and (21) we used the fact that $\rho_c s_c = b_{2_c}/2$ and $\rho_r s_r = b_{2_r}/2$ [see Eq. (2)]. Equation (19) is the general form of the acceleration experienced by a compound sail with optical properties. The force coefficients $\mathcal{B}$ and $\mathcal{C}$ are only functions of the optical properties of the reflecting material, whereas $\mathcal{A}$ also depends on the collector geometry through the aperture angle ξ_0.

Note that in the ideal case ($\mathcal{A}=0$, $\mathcal{B}=2$, and $\mathcal{C}=0$) Eq. (19) reduces to the well-known result

$$\boldsymbol{a} = (2PA_p/m)\cos\alpha\hat{\boldsymbol{n}}_d \tag{22}$$

which states that the acceleration is proportional to the cosine of the cone angle α.

A comparison between the acceleration experienced by a conventional flat sail [see Eq. (1)] and that of a compound sail [see Eq. (19)] reveals that the latter has the same structure of the former except for the term $\cos\alpha$. This is exactly the difference between conventional and compound sails in the ideal case.

Having established a dependence of the compound sail acceleration on the optical properties of its components, it is useful to investigate different scenarios where various approximations are compared. In particular, we distinguish between three cases with increasing differences of the sailcraft with respect to an ideal model. As a first approximation, we consider a model (referred to as OC-IR-ID) with an optical behavior of the collector and ideal characteristics for both the reflector and the director. The second case (OC-OR-ID) assumes an optical behavior of both the collector and the reflector and an ideal director. The last case (OC-OR-OD) assumes an optical behavior for all of the three components. Because the collector area is much greater than the areas of both the reflector and the director, it is reasonable to conclude that the OC-IR-ID represents a realistic mathematical model for an optical compound sail. In fact the losses caused by nonperfect reflectivity of the reflector and director are likely to be taken under control through a suitable design of their optics and/or using reflecting materials with better optical properties. Nevertheless, the other two approximations (OC-OR-ID and OC-OR-OD cases) can be thought of as representing a lower bound to the obtainable performance with a nonideal compound sail.

For a fixed value of ξ_0, the greater are the differences with respect to the ideal case, the greater is the value of the coefficient $\mathcal{A}$ and, correspondingly, the radial component of the acceleration [see Eq. (19)]. The force coefficients $\mathcal{A}$, $\mathcal{B}$, and $\mathcal{C}$ are computed in Table 1 under the assumption that the characteristics of the reflective film correspond to a Jet Propulsion Laboratory square sail[7] and $\xi_0 = 15$ deg.

Figure 3 shows the normalized acceleration modulus of the compound sail $a/(2PA_p/m)$ as a function of the cone angle α for various sail models using the coefficients of Table 1. Unlike conventional sails, when the optical properties of the compound sail are taken into account there exists a critical cone angle α^* beyond which the sailcraft acceleration is greater than that corresponding to an ideal model. In fact, unlike the ideal case in each optical model the sailcraft acceleration is different from zero for all of the values of the cone angle (included $\alpha = 90$ deg) as long as $b_{2_c} \neq 0$. This is because of the difference between the resultant force acting on the collector and that on the director. This differential force is directed along the

Table 1 Force coefficients $\mathcal{A}$, $\mathcal{B}$, and $\mathcal{C}$ for a compound sail with different approximation models and a spread angle $\xi_0 = 15$ deg

Coefficient	Ideal sail	OC-IR-ID	OC-OR-ID	OC-OR-OD
$\mathcal{A}$	0	0.1621	0.3042	0.4225
$\mathcal{B}$	2	1.6544	1.3685	1.1320
$\mathcal{C}$	0	0	0	−0.0075

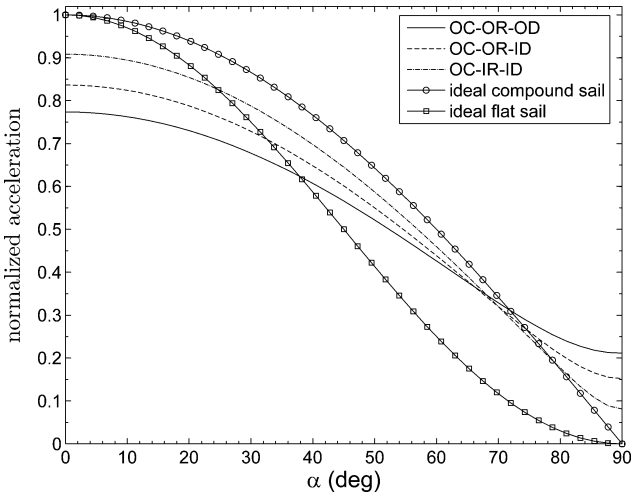

Fig. 3 Acceleration of the compound sail (normalized by the maximum acceleration for the ideal model) as a function of the cone angle α.

collector axis and cannot be counterbalanced by the force on the director whatever the cone angle is. From a practical standpoint this means that coast arcs are not allowed in the trajectories.

The value of the critical angle is easily obtained equating Eqs. (19) and (22) and solving for α. The result is

$$\cos\alpha^* = \frac{-\mathcal{C}(\mathcal{A}+\mathcal{B}) - \sqrt{\mathcal{C}^2\mathcal{A}^2 - \mathcal{B}^2\mathcal{A}^2 + 4\mathcal{A}^2 + 4\mathcal{C}^2 - 2\mathcal{A}^3\mathcal{B}}}{\mathcal{B}^2 + 2\mathcal{A}\mathcal{B} - 4} \tag{23}$$

Assuming $\xi_0 = 15$ deg, one has $\alpha^* \cong 68$ deg for the OC-IR-ID model, $\alpha^* \cong 66$ deg for the OC-OR-ID model, and $\alpha^* \cong 72$ deg for the OC-OR-OD model.

Control Law for Minimum-Time Problem

The equations of motion for a compound sail in a heliocentric inertial frame $\mathcal{T}_\odot(x, y, z)$ are

$$\dot{\boldsymbol{r}} = \boldsymbol{v} \tag{24}$$

$$\dot{\boldsymbol{v}} = -\left(\mu_\odot / r^3\right)\boldsymbol{r} + \boldsymbol{a} \tag{25}$$

where $[\boldsymbol{r}]_{\mathcal{T}_\odot} = [r_x, r_y, r_z]^T$ and $[\boldsymbol{v}]_{\mathcal{T}_\odot} = [v_x, v_y, v_z]^T$ are the spacecraft position and velocity relative to $\mathcal{T}_\odot$, $\mu_\odot$ is the sun's gravitational parameter, and $\boldsymbol{a}$ is the acceleration caused by the solar radiation pressure P. The dependence of the acceleration on the distance from the sun is more conveniently expressed through the introduction of the lightness number β, that is, the ratio of the maximum acceleration caused by solar photons on an ideal compound sail (at a given distance r from the sun) to the corresponding sun's gravitational acceleration. In other terms $\beta = (2PA_p)/(\mu_\odot/r^2)$. Introducing β into Eq. (19) yields

$$\boldsymbol{a} = \left(\beta\mu_\odot / 2r^2\right)[\mathcal{A}\hat{\boldsymbol{r}} + (\mathcal{B}\cos\alpha + \mathcal{C})\hat{\boldsymbol{n}}_d] \tag{26}$$

Let $\mathcal{T}_{\text{orb}}(x_{\text{orb}}, y_{\text{orb}}, z_{\text{orb}})$ be an orbital frame with unit vectors $\hat{\boldsymbol{i}}_{\text{orb}} \equiv \hat{\boldsymbol{r}}$, $\hat{\boldsymbol{j}}_{\text{orb}}$, and $\hat{\boldsymbol{k}}_{\text{orb}}$. Assume that the plane $z_{\text{orb}} = 0$ contains the axis z of the $\mathcal{T}_\odot$ frame and $\hat{\boldsymbol{j}}_{\text{orb}}$ points toward the ecliptic pole. Recall that $\hat{\boldsymbol{n}}_d$ in Eq. (26) is the unit vector normal to the director, $\alpha \in [0, \pi/2]$ is the director's sail cone angle, and $\delta \in [-\pi, \pi]$ is the corresponding sail clock angle (positive in the counterclockwise direction). Then

$$[\hat{\boldsymbol{n}}_d]_{\mathcal{T}_{\text{orb}}} = [\cos\alpha, \sin\alpha\cos\delta, \sin\alpha\sin\delta]^T \tag{27}$$

The problem is to find the optimal control law $\boldsymbol{u}(t) = [\alpha(t), \delta(t)]^T$ (where $t \in [0, t_f]$), which minimizes the time t_f necessary to transfer the spacecraft from an initial $(\boldsymbol{r}_0, \boldsymbol{v}_0)$ to a final $(\boldsymbol{r}_f, \boldsymbol{v}_f)$ prescribed state. This amounts to maximizing the performance index:

$$J = -t_f \tag{28}$$

From Eqs. (24) and (25) the Hamiltonian of the system is

$$H = \boldsymbol{\lambda}_r \cdot \boldsymbol{v} - \left(\mu_\odot / r^3\right)\boldsymbol{\lambda}_v \cdot \boldsymbol{r} + \boldsymbol{\lambda}_v \cdot \boldsymbol{a} \tag{29}$$

where $\boldsymbol{\lambda}_r \triangleq [\lambda_{r_x}, \lambda_{r_y}, \lambda_{r_z}]^T$ and $\boldsymbol{\lambda}_v \triangleq [\lambda_{v_x}, \lambda_{v_y}, \lambda_{v_z}]^T$ are the vectors adjoint to the position and the velocity, respectively. The components of the primer vector $\boldsymbol{\lambda}_v$ in the $\mathcal{T}_{\text{orb}}$ frame are given by

$$[\boldsymbol{\lambda}_v]_{\mathcal{T}_{\text{orb}}} = \lambda_v[\cos\alpha_\lambda, \sin\alpha_\lambda, \cos\delta_\lambda, \sin\alpha_\lambda\ \sin\delta_\lambda]^T \tag{30}$$

where $\lambda_v = \|\boldsymbol{\lambda}_v\|$, whereas $\alpha_\lambda \in [0, \pi]$ and $\delta_\lambda \in [-\pi, \pi]$ are the primer vector cone and clock angle, respectively.

The derivatives of the Hamiltonian with respect to $\boldsymbol{r}$ and $\boldsymbol{v}$ provide the expressions of the Euler–Lagrange equations. As a result, one has

$$\begin{aligned}\dot{\boldsymbol{\lambda}}_r = {} & \left(\mu_\odot / r^3\right)\boldsymbol{\lambda}v - \left(3\mu_\odot / r^3\right)(\boldsymbol{\lambda}_v \cdot \hat{\boldsymbol{r}})\hat{\boldsymbol{r}} - \left(\beta\mu_\odot / 2r^3\right) \\ & \times \{\mathcal{A}[\boldsymbol{\lambda}_v - 3(\boldsymbol{\lambda}_v \cdot \hat{\boldsymbol{r}})\hat{\boldsymbol{r}}] + \mathcal{B}(\boldsymbol{\lambda}_v \cdot \hat{\boldsymbol{n}}_d)[\hat{\boldsymbol{n}}_d - 3(\hat{\boldsymbol{n}}_d \cdot \hat{\boldsymbol{r}})\hat{\boldsymbol{r}}] \\ & - 2\mathcal{C}(\boldsymbol{\lambda}_v \cdot \hat{\boldsymbol{n}}_d)\hat{\boldsymbol{r}}\}\end{aligned} \tag{31}$$

$$\dot{\boldsymbol{\lambda}}_v = -\boldsymbol{\lambda}_r \tag{32}$$

The boundary conditions for the sailcraft position and velocity are constrained by the planetary ephemerides at both departure and arrival. In particular, at the end of the trajectory one has

$$\boldsymbol{r}_f = \boldsymbol{r}^{(p)}(t_f), \qquad \boldsymbol{v}_f = \boldsymbol{v}^{(p)}(t_f) \tag{33}$$

where $\boldsymbol{r}^{(p)}$ and $\boldsymbol{v}^{(p)}$ are the position and velocity of the target planet. Observing that $\dot{\boldsymbol{r}}^{(p)}(t_f) = \boldsymbol{v}_f$ and $\dot{\boldsymbol{v}}^{(p)}(t_f) = -\mu_\odot \boldsymbol{r}_f / r_f^3$, the transversality condition is given by[8]

$$H(t_f) = 1 + \boldsymbol{\lambda}_r(t_f) \cdot \boldsymbol{v}_f - \left(\mu_\odot / r_f^3\right)\boldsymbol{\lambda}_v(t_f) \cdot \boldsymbol{r}_f \tag{34}$$

From the Pontryagin's maximum principle, the optimal control law $\boldsymbol{u}(t)$, to be selected in the domain of feasible controls $\mathcal{U}$, is such that, at any time, the Hamiltonian is an absolute maximum. Let

$$H' \triangleq \left(\beta\mu_\odot / 2r^2\right)[\mathcal{B}(\hat{\boldsymbol{n}}_d \cdot \hat{\boldsymbol{r}}) + \mathcal{C}](\hat{\boldsymbol{n}}_d \cdot \boldsymbol{\lambda}_v) \tag{35}$$

be that portion of the Hamiltonian H that explicitly depends on the control vector. Then the optimal control law is such that

$$\boldsymbol{u} = \arg\max_{u \in \mathcal{U}} H \equiv \arg\max_{u \in \mathcal{U}} H' \tag{36}$$

Substituting Eqs. (27) and (30) into Eq. (35) and setting it to zero, the derivative $\partial H'/\partial \boldsymbol{u}$ yields

$$\alpha_\lambda = \alpha + \tan^{-1}\left(\frac{\mathcal{B}\sin\alpha}{\mathcal{B}\cos\alpha + \mathcal{C}}\right) \tag{37}$$

$$\tan\delta = \tan\delta_\lambda \tag{38}$$

Equation (37) is an extension of a similar result found for an ideal compound sail. In fact, letting $\mathcal{C} = 0$ (which corresponds to an ideal case) the control law reduces to $\alpha = \alpha_\lambda/2$ and coincides with the result in Ref. 3. Note, however, that $\mathcal{C} = 0$ is representative not only of the ideal case, but also of cases OC-IR-ID and OC-OR-ID (see Table 1).

Consider now a director having nonideal properties (case OC-OR-OD). Substituting Eqs. (27) and (30) into Eq. (36), one obtains the values of the cone angle for which H' is greater than or equal to zero. Because $H' = 0$ implies either $\hat{\boldsymbol{n}}_d \cdot \boldsymbol{\lambda}_v = 0$ (that is, $\alpha = \alpha_\lambda - \pi/2$) or $\mathcal{B}(\hat{\boldsymbol{n}}_d \cdot \hat{\boldsymbol{r}}) + \mathcal{C} = 0$ [that is, $\alpha = \cos^{-1}(-\mathcal{C}/\mathcal{B})$], the following result is obtained:

$$\begin{aligned}H' \geq 0 \Rightarrow {} & [\alpha \geq \alpha_\lambda - \pi/2 \cap \alpha \leq \cos^{-1}(-\mathcal{C}/\mathcal{B})] \\ & \cup [\alpha \leq \alpha_\lambda - \pi/2 \cap \alpha \geq \cos^{-1}(-\mathcal{C}/\mathcal{B})]\end{aligned} \tag{39}$$

The situation is illustrated in Fig. 4 using the force coefficients given in Table 1. In particular, it shows that all of the pairs (α, α_λ) in Eq. (37) satisfy the Legendre–Clebsch condition.

To summarize, Eq. (37) gives the optimal cone angle α as a function of α_λ and of the compound sail parameters $\mathcal{B}$ and $\mathcal{C}$. As long as OC-IR-ID or OC-OR-ID models are considered, the optimal control law coincides with that of the ideal case because $\mathcal{C} = 0$. This is no longer true for OC-OR-OD. However, because $|\mathcal{C}/\mathcal{B}| \ll 1$, Eq. (37)

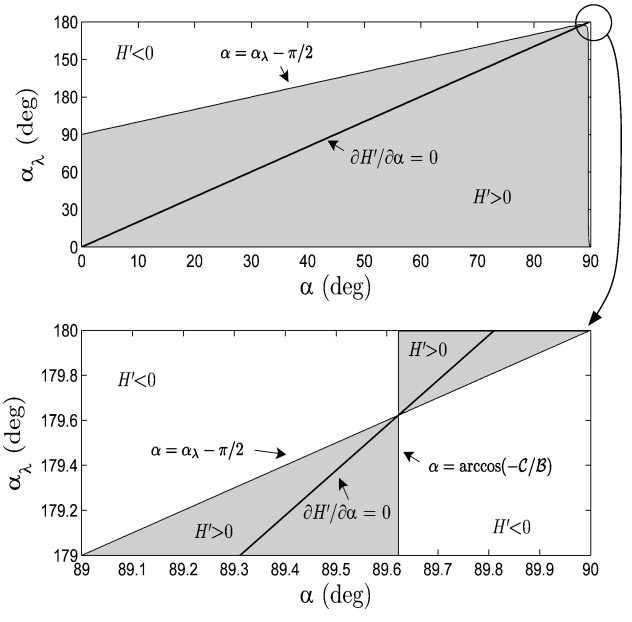

Fig. 4 Optimal cone angle α for a compound solar sail.

indicates that $\alpha \cong \alpha_\lambda/2$, that is, the optimal control law is nearly identical to that corresponding to an ideal compound sail.

Finally, note from Eq. (38) that the unit vector normal to the director $\boldsymbol{n}_d$ lies in the plane defined by the position vector and the primer vector. This is a generalization of a similar result found for a nonideal solar sail[5] and an ideal compound sail.[3]

Illustrative Results

The optical force model for a compound sail and the corresponding control law described earlier have been applied to study the heliocentric phase of transfer missions to Mars and Venus. All of the simulated trajectories are characterized by zero values of hyperbolic excess velocity at both endpoints. The force coefficients $\mathcal{A}$, $\mathcal{B}$, and $\mathcal{C}$ are given in Eqs. (20) and (21), and the corresponding numerical values are those in Table 1.

A set of canonical units has been used in the integration of the differential equations to reduce their numerical sensitivity. The differential equations have been integrated in double precision using a Runge–Kutta fifth-order scheme with absolute and relative errors of 10^{-12}. The boundary-value problem associated with the variational problem has been solved through a hybrid numerical technique combining genetic algorithms (to obtain an estimate of the adjoint variables), with gradient-based and direct methods to refine the solution.[5]

As a preliminary step, the optimal (minimum time) trajectories for Mars and Venus missions have been studied in a two-dimensional framework, assuming circular and coplanar planetary orbits. When the final polar angle of the sailcraft (measured from some reference position) is left free in the optimization process, the planar model allows one to obtain an estimate of the minimum attainable transfer time for a given value of the lightness number β. Results are shown for Mars (Fig. 5) and Venus (Fig. 6) missions as a function of β. Both figures show similar trends for the various approximation models. In particular, it should be noted that for both Mars and Venus missions the OC-IR-ID model offers performance very close to that attainable with a flat ideal sail. This is an interesting result in that, as already discussed, the OC-IR-ID model represents a realistic mathematical model for a compound sailcraft.

Optimum rendezvous data for these two planets have also been extended to a three-dimensional problem using their actual orbital elements. In this study the boundary conditions are constrained by the planetary ephemerides based on the JPL DE405/LE405 model.[9] Assuming lightness numbers $\beta = 0.2$ and 0.4, Fig. 7 shows the results obtained for a Mars mission when the starting date, expressed in terms of modified Julian date (MJD), is varied in the range September 2009–January 2010. The performance data for Mars transfer present a nonnegligible difference with the two-dimensional case, on the order of 40 days, because of the orbital eccentricity of this planet. Note that the minimum transfer times for ideal and optical compound models are obtained with very similar starting dates. (In all cases the minima are around 10 November 2009 when $\beta = 0.2$ and 25 December 2009 when $\beta = 0.4$.) The minimum transfer times with a OC-IR-ID model (417 days when $\beta = 0.2$ and 344 days when $\beta = 0.4$) are only 10% greater than those obtained with an ideal model.

For Venus missions, assuming again $\beta = 0.2$ and 0.4, Fig. 8 shows the mission times around the minima when the starting date is varied

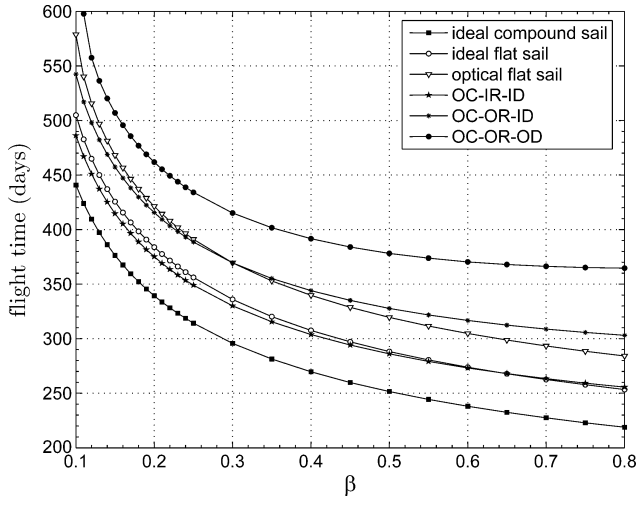

Fig. 5 Minimum mission times for circular, coplanar rendezvous to Mars.

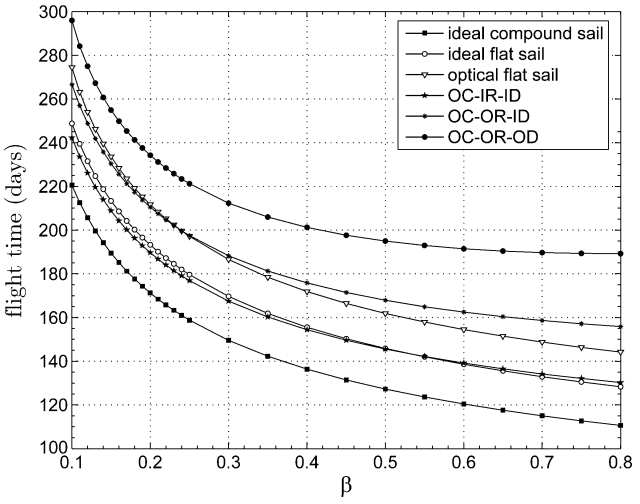

Fig. 6 Minimum mission times for circular, coplanar rendezvous to Venus.

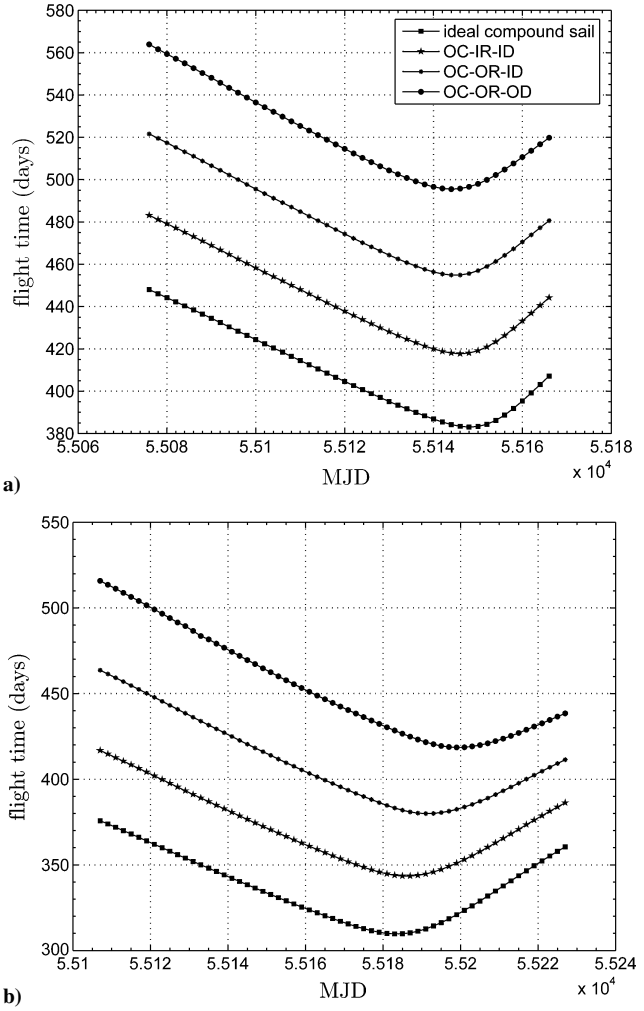

Fig. 7 Flight times for a Mars mission (three-dimensional problem) with ideal and optical compound sail: β = a) 0.2 and b) 0.4.

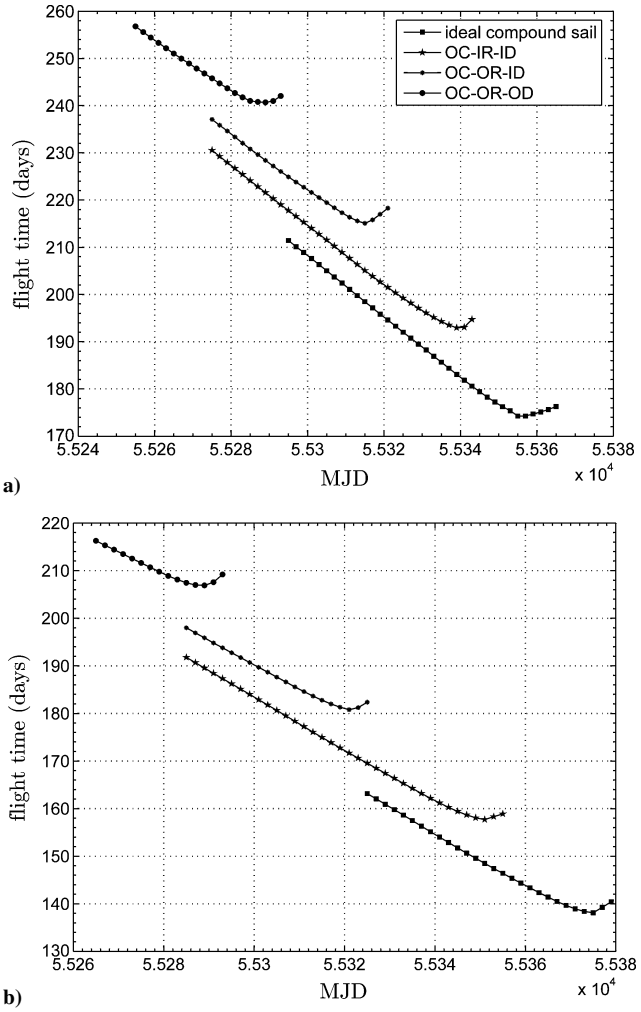

Fig. 8 Flight times for a Venus mission (three-dimensional problem) with ideal and optical compound sail: β = a) 0.2 and b) 0.4.

in the range February–June 2010. In this case the starting dates to get optimal transfer times are quite different for the four models. However, the minima are in excellent agreement with the results obtained in the two-dimensional case (Fig. 6). This is because of the small values of both eccentricity and inclination of the Venusian orbit. The mission times for a compound sail with the OC-IR-ID model are 193 days when $\beta = 0.2$ and 157 days when $\beta = 0.4$, with an increase of 12% with respect to the ideal case.

Conclusions

A compound solar-sail model, in which the optical properties of the collector, reflector, and director have been taken into account, has been investigated. A compact expression for the resultant force acting on the sailcraft has been derived in which two force coefficients depend only on the optical properties of the reflecting material, whereas the third one also depends on the collector geometry. Unlike the ideal case, the sailcraft acceleration is different from zero for any cone angle. This new model allows one to establish a more realistic comparison between the performance attainable with conventional and compound solar sails. To this end, the optimal control law for minimum-time three-dimensional interplanetary trajectories has been solved using an indirect approach. The resulting steering law generalizes a similar result available for an ideal compound sail. Applications to transfers toward Mars and Venus have been discussed. Assuming that the main losses of the compound sail are concentrated in the collector, the minimum transfer times obtainable with a compound sail are shorter than those of a conventional sail with optical properties and are close to those of an ideal flat sail. As there exists a critical cone angle beyond which the sailcraft acceleration of the optical model is greater than that with an ideal model, even better performance of compound sails are expected for those missions requiring high values of cone angles.

We finally note that a fully realistic comparison between conventional and compound solar sails needs a more detailed study. In fact, it is likely that the compound sail will have a significant mass penalty compared to a flat sail because of the mass of the additional mirrors and the structure required to join them together. An important issue would be to determine the payload mass delivered for a given launch mass, taking into account both trajectory optimization and the mass budget of the flat and compound sails. This is beyond the scope of the current Note and is left to future research.

References

[1]Forward, R. L., "Solar Photon Thrustor," *Journal of Spacecraft and Rockets*, Vol. 27, No. 4, 1990, pp. 411–416.

[2]McInnes, C. R., "Payload Mass Fractions for Minimum-Time Trajectories of Flat and Compound Solar Sails," *Journal of Guidance, Control, and Dynamics*, Vol. 23, No. 6, 2000 pp. 1076–1078.

[3]Mengali, G., and Quarta, A. A., "Time-Optimal Three-Dimensional Trajectories for Solar Photon Thruster Spacecraft," *Journal of Spacecraft and Rockets*, Vol. 42, No. 2, 2005, pp. 379–381.

[4]Mengali, G., and Quarta, A. A., "Earth Escape by Ideal Sail and Solar-Photon Thrustor Spacecraft," *Journal of Guidance, Control, and Dynamics*, Vol. 27, No. 6, 2004, pp. 1105–1108.

[5]Mengali, G., and Quarta, A. A., "Optimal Three-Dimensional Interplanetary Rendezvous Using Nonideal Solar Sail," *Journal of Guidance, Control, and Dynamics*, Vol. 28, No. 1 2005, pp. 173–177.

[6]Flint, E. M., "Robert L. Forward's Solar Photon Thruster Solar Sail Architecture Revisited," AIAA Paper 2004-1578, April 2004.

[7]McInnes, C. R., *Solar Sailing: Technology, Dynamics and Mission Applications.* Springer-Praxis Series in Space Science and Technology, Springer-Verlag, Berlin, 1999, pp. 32–55.

[8]Lewis, F. L., *Optimal Control*, Wiley, New York, 1986, pp. 235, 236.

[9]Pitjeva, E. V., "Modern Numerical Ephemerides of Planets and the Importance of Ranging Observations for Their Creation," *Celestial Mechanics and Dynamical Astronomy*, Vol. 80, No. 3, 2001, pp. 249–271.

D. Spencer
Associate Editor